

Effect of mass and center of gravity on vehicle speed and braking performance

Jack Tian¹ and Clifford Whitfield²

¹Troy High School, Fullerton, CA

²Department of Mechanical and Aerospace Engineering, The Ohio State University, Columbus, OH

SUMMARY

The center of gravity (CG) of a vehicle is a key parameter that helps determine vehicle stability, braking efficiency, and safety. In a gravity vehicle, the mass of the vehicle is also an important factor in vehicle performance because it provides the sole force of propulsion. We hypothesized that if a vehicle was constructed according to mathematically-derived optimal mass and CG location, then a fast and accurate vehicle would result. To test this hypothesis, we constructed a gravity vehicle, which is a vehicle powered by its own gravity on a ramp. Mathematical calculations were used to rationalize this hypothesis. Shifting the CG rearward increased the vehicle's effective launching height on the ramp and corresponding gravitational potential energy, resulting in greater kinetic energy and speed. However, the accuracy (m^{-1}), defined as the reciprocal of braking distance from the target, increased initially, peaked, and then decreased as the vehicle mass increased. We performed experiments with five mass parameters and three load locations, using an unloaded vehicle as control. Speed and accuracy were then measured for 16 sets of data. Compared to front and centrally-loaded vehicles, the rear-loaded vehicles displayed the best results. As the mass increased to a medium value, both the speed and accuracy reached a maximum. The experimental results supported the hypothesis that the optimal CG position is 22 ± 1 cm rear of the front axle and the ideal mass is 867 ± 50 grams. This study highlights the significance of CG position in vehicle design.

INTRODUCTION

The center of gravity (CG) is a critical parameter that impacts vehicle handling, since the CG position in each spatial axis affects the vehicle's stability, ride comfort and safety. Accordingly, it is crucial for calculations of vehicle performance parameters. In this study, we developed a model to determine the optimal vehicle mass and CG location for a fast gravity vehicle with high braking accuracy. We drew on previously reported methods including algorithms, software-based model simulations, real-time estimates and more, to determine the optimal CG location. Previous studies reported that moving the battery pack along the electric vehicle significantly impacted the mass distribution (1). A model-based simulation using MATLAB SIMULINK was presented

to demonstrate the effect of changing CG position on vehicle stability (1). Albeit with different purpose, this study formed the basis of our hypothesis. Other vehicle parameters were also informed by previous studies. For example, a study on vehicle load found that an increase in CG height results in a decrease in maximum driving speed since stability decreases as CG height increases (2). Therefore, in order to minimize the adverse impact of the height of CG on vehicle stability, the vehicle was designed to move as closely as possible to the ground. Skrucany *et al.* investigated the influence of cargo weight and its position on brakes. They demonstrated that loads should be as close to the ground and rear axle as possible to reduce the braking distance (3, 4). These considerations were also taken into account in the design of the vehicle. We drew on models developed by Mehmet *et al.* (5) in order to optimize the height, horizontal position, and lateral position of the CG of a vehicle. We designed the vehicle braking system for optimal braking accuracy. Lee *et al.* proposed a practical algorithm for estimating a vehicle's longitudinal CG location in real time, and its viability was verified through simulations and experiments using a test vehicle equipped with electro-mechanical brakes on the rear wheels (6). The braking concept in this report helped in designing an efficient braking system.

From these studies, we gained insight into how to construct a fit-for-purpose gravity vehicle. We chose smaller wheels to lower the height of the CG, and we used a lightweight, symmetric, and even basswood board as the chassis so that the lateral CG was located on the center line. However, the most important takeaway from the previous studies was that a rearward shift in CG could significantly increase braking accuracy.

During vehicle construction, it became apparent that the vehicle's mass and CG position would impact the vehicle's speed and accuracy. With a vehicle in hand, we asked two questions: What was the optimal mass and where was the best CG location? In the ready-to-launch position, the vehicle was hung vertically on the bolt of the trigger. Accordingly, a rearward CG would theoretically result in a greater starting height and potential energy, which is converted to higher departure speed at the bottom of the ramp. Previous studies showed that a CG location as close as possible to the rear axle not only increased vehicle stability, but also significantly reduced braking distance (3, 4). Based on these conclusions, we predicted that the best CG location would be close to the vehicle's rear axle. On the other hand, when the vehicle reaches the desired speeds through manipulation of the CG towards the rear, the vehicle mass becomes a crucial factor in its accuracy. With greater mass, there is greater momentum, which could exceed braking endurance and cause vehicle



Figure 1: Gravity Vehicle with Different Mass Loading. (A) The front load was located behind the front axle due to the dowel in front of the axle. (B) The load was located at the middle point of the vehicle length, and the load behind the rear axle. All three load configurations were located on the center line and secured with duct tape to prevent movement during the run.

skidding. We therefore hypothesized that a medium-mass vehicle might display the best braking accuracy. To rationalize the two hypotheses, we built physics models for the analysis of energy conversion and braking forces. From the model studies, we concluded that a medium-mass vehicle with the rearward CG would have high speed and accuracy. We performed trials with five mass parameters and three location variables, along with the unloaded vehicle as a control. We graphed the resulting data to determine how CG position and vehicle mass impact the accuracy and speed.

RESULTS

We conducted the experiments that obtained the optimal mass and CG location with a gravity vehicle device, which uses the vehicle's gravitational potential energy on a ramp as the sole means of propulsion to arrive at a target as quickly and accurately as possible. We built a ramp with a height of no more than 100.0 centimeters and a 50.0 cm x 50.0 cm base, as well as a vehicle with a mass of no more than 2.000 kilograms (7). The target was arranged between 9.00 to 12.00 meters away from the bottom of the ramp. Both the run time and braking distance were measured to evaluate vehicle performance. The vehicle speed was calculated as the distance traveled by the vehicle divided by the time measured from the launch to the end of the vehicle's run. A round wooden dowel was attached to the front of the vehicle. The braking distance was measured from the dowel's front bottom edge to the center of the target. To facilitate comparison of braking performance, the concept of accuracy (m^{-1}) was introduced by dividing 100 by the braking distance (m). The shorter the

braking distance, the higher the vehicle accuracy.

With an unloaded vehicle (507 grams) as a control, 120 grams of load (mass + tape) were added on three positions on the vehicle: the front, middle and rear (**Figure 1**), to investigate their impact on vehicle behavior. The rear loadings yielded the best results compared with corresponding middle and rear loadings of the same mass (**Table 1**). We observed a trend where both accuracy and speed are independent of the vehicle's mass, increasing as the CG position was moved rearward (**Figure 2A & 2B**). On the other hand, as the vehicle mass was increased from 507 to 867 grams, both accuracy and speed increased for all masses of vehicle. However, further increases of the vehicle mass from 867 to 1107 grams resulted in a decrease in accuracy while the speed remained unchanged. The CG was shifted away from the front axle as the mass load was moved from the front to the middle to the rear location (**Table 1**). Increasing the mass in the rear from 627 to 1107 grams strengthened the rearward trend of the CG.

Plotting the accuracy against vehicle mass (**Figure 3A**) resulted in an approximately normal distribution. When the mass load of 360 grams was placed onto the rear part of the vehicle, the greatest accuracy was achieved (**Table 1**). Meanwhile, graphing the speed against vehicle mass (**Figure 3B**) produced an S-shape curve with a peak, indicating that when the mass was beyond 867 grams, the speed had reached its maximum. Compared to the unloaded control, the vehicle with a mass of 867 grams and rear loading displayed an 89% increase in accuracy and a 26% increase in speed. These experimental results support the hypothesis that the

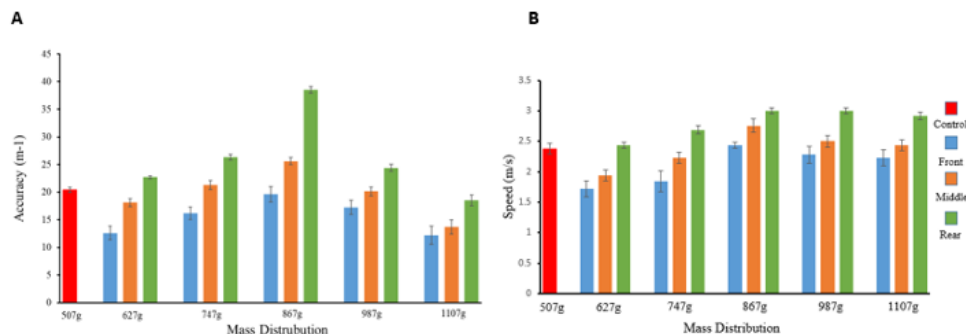


Figure 2: Effect of CG Location on Accuracy and Speed. The average (A) accuracy (m^{-1}) and (B) speed (m/s) of (specify) was measured for 6 different weights of a gravity vehicle (507, 627, 747, 867, 987, and 1107 g) as the load was moved from the front (blue), middle (orange), and rear (green) of the vehicle. Measurements were compared to an unloaded vehicle as a control (red) ($n = 3$). Error bars represent two standard deviations.

Vehicle Mass (grams)	Loading Mass Location	CG Distance from Front Axle (cm)	Results			
			Average Distance (cm)	Accuracy (m ⁻¹)	Average Time (s)	Speed (m/s)
507	None	14.0	4.9	20.4	4.4	2.39
627	F	11.9	7.9	12.6	6.1	1.72
	M	14.2	5.5	18.1	5.4	1.94
	R	17.6	4.4	22.7	4.3	2.44
747	F	10.5	6.2	16.1	5.6	1.85
	M	14.3	4.7	21.3	4.7	2.23
	R	20.1	3.8	26.3	3.9	2.69
867	F	9.5	5.1	19.6	4.4	2.39
	M	14.3	3.9	25.6	3.8	2.76
	R	21.9	2.6	38.5	3.5	3.00
987	F	8.7	5.8	17.2	4.6	2.28
	M	14.4	5.0	20.0	4.2	2.50
	R	23.2	4.1	24.4	3.5	3.00
1107	F	8.1	8.2	12.2	4.7	2.23
	M	14.4	7.3	13.7	4.3	2.44
	R	24.3	5.4	18.5	3.6	2.92

Table 1: Vehicle's Mass and CG Location Effects on Accuracy and Speed. Accuracy (m⁻¹) was calculated by dividing 100 by average distance (m) from target while speed (m/s) was calculated as 10.5 m/average runtime (s). *F* represents the front location, *M* the middle location, and *R* the rear location. Every data value was obtained as an average from 3 trials.

vehicle with medium mass and CG position as close as possible to the rear axle would have the best performance.

DISCUSSION

Besides low friction, there are two main considerations with the ramp design: fast vehicle descent and efficient direction change. The vehicle gains speed from gravity and changes its direction of movement from downwards at the top of the ramp top to forward at the bottom of the ramp. A Brachistochrone curve meets these requirements, providing the theoretical shortest time in rolling from the top to the bottom of the ramp (8). The descent time has an integration relationship with the curve function $y(x)$ as shown in Equation (1):

$$T = \int_0^x \frac{\sqrt{1+y'^2}}{\sqrt{2gy}} dx \quad (1)$$

where y' is the derivative of x and g represents the acceleration of gravity. To compromise short descent time and seamless connection between the ramp and floor, the ramp surface was made in the shape of a modified Brachistochrone curve.

As the gravity vehicle rolls down the ramp, gravitational potential energy is converted into translational and rotational kinetic energy. The vehicle moves on the track until it brakes at the target. During the braking process, the kinetic energy of the vehicle is converted into elastic potential energy stored in

the torsion spring. The torsion spring functions as an energy storage by generating negative torque to oppose the motion of the vehicle (9). After each run, the energy stored in the spring is released manually so that another run can start. Each run of the vehicle involves the Law of Energy Conservation. If energy loss is negligible, gravitational potential energy of the vehicle is fully converted into the elastic potential energy stored in the torsion spring (Figure 4). The vehicle that starts from the rest at the top of the ramp and stops at the target functions as an energy carrier. After each experiment, the energy stored in the spring is released manually so that another experiment can start.

Analysis of the vehicle's energy conversion provides theoretical evidence for the optimal vehicle mass range. When the trigger is pressed and the gravity vehicle rolls down the ramp, it undergoes changes in its energy state. Based on the Law of Energy Conservation, the vehicle's gravitational potential energy is converted into kinetic energy since the energy loss from air resistance is negligible. The energy conservation equation is shown as:

$$K_i + U_i = K_f + U_f \quad (2)$$

In this equation, the initial kinetic energy $K_i = 0$ and the final potential energy $U_f = 0$ of the bottom of the ramp are chosen as the references. Replacing U_i with MgH and K_f with translational ($\frac{1}{2}Mv^2$) and rotational ($\frac{1}{2}I\omega^2$) kinetic energy,

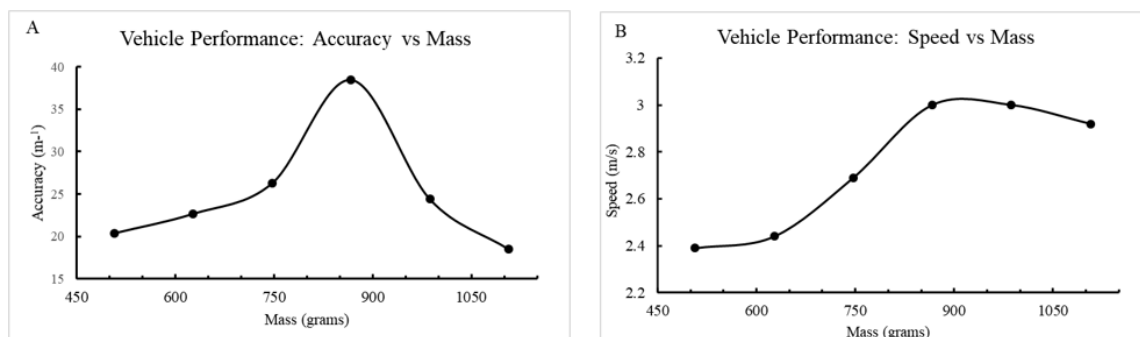


Figure 3: Vehicle Mass Effect on Accuracy and Speed. (A) The average (A) accuracy (m⁻¹) and (B) speed (m/s) of (specify) was measured for 6 different weights of a gravity vehicle (507, 627, 747, 867, 987, and 1107 g).

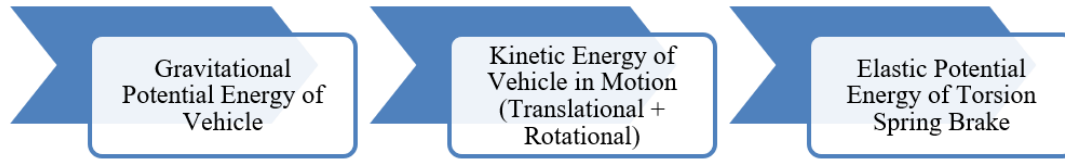


Figure 4: Energy Conversion of Gravity Vehicle. In each experiment, the gravity vehicle converts its own gravitational potential energy at the ramp top to kinetic energy in motion to elastic potential energy stored in the torsion spring.

where M is the vehicle mass, H is the launching height of the vehicle, v is the translational speed, I is the moment of inertia, and ω is the rotational speed. Equation (2) can be simplified as:

$$MgH = \frac{1}{2}Mv^2 + \frac{1}{2}I\omega^2 \quad (3)$$

Equation (3) shows that the vehicle's gravitational potential energy is converted into its translational speed (v) and rotational speed (ω). ω is proportional to v , in which R is the wheel radius. Since the body of the vehicle is not rotating, only the mass (m) of the wheels, axles and shafts contribute to the moment of inertia of the vehicle. Introducing, Equation (3) can be written as:

$$MgH = \frac{1}{2}Mv^2 + \frac{1}{2}(\frac{1}{2}mR^2)(\frac{v}{R})^2 \quad (4)$$

and solved for velocity:

$$v = \sqrt{\frac{MgH}{\frac{1}{2}M + \frac{1}{4}m}} = \sqrt{\frac{gH}{\frac{1}{2} + \frac{m}{4M}}} \quad (5)$$

From Equation (5), assuming the friction is negligible when the vehicle slides down the ramp ($m = 0$), it will get the maximum speed: $v = \sqrt{2gH}$.

In contrast, when the nonrotating body mass is very small compared to rotating mass ($m \approx M$), the vehicle gets minimum speed $v = \sqrt{\frac{4gH}{3}}$.

In any case, we can conclude that a greater starting height (H) will increase the translational speed (v). Equation (5) also shows that as the total mass (M) increases, the vehicle speed increases when it arrived at the ramp bottom. However,

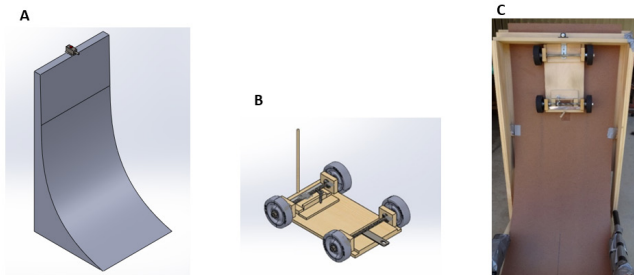


Figure 5: Gravity Vehicle Device. (A) CAD model of ramp created by SOLIDWORKS. The ramp fits within a rectangular box with a 50.0 cm x 50.0 cm base and a height of 100.0 cm. (B) CAD model of vehicle created with SOLIDWORKS. The vehicle has a dowel in the front for timing by photogate and a U-bolt plate in the rear for hanging on the trigger. (C) Ready-to-launch gravity vehicle. The gravity vehicle is hung at the top of the ramp. When the trigger button is pressed, the vehicle accelerates down the ramp due to its own gravity. The vehicle achieves maximum speed at the bottom.

this is the opposite to the vehicle moving on the track since the friction force (μMg) which decelerates the vehicle is proportional to the mass. A medium mass (M) achieves the best balance between these two opposing forces and yields the maximum speed. In addition, the greater the total mass (M) of the vehicle, the greater the momentum of the vehicle (p), as related by the equation:

$$p = Mv \quad (6)$$

A heavier vehicle has greater momentum, thus making it harder to brake. Based on Equations (5) and (6), we hypothesized that a medium-mass vehicle would give the best results because the mass must be decreased to reduce momentum without sacrificing speed. As the vehicle stops at the target, its kinetic energy is converted into elastic potential energy stored in the torsion spring. The conversion obeys the following energy

$$\frac{1}{2}Mv^2 + \frac{1}{2}I\omega^2 = \frac{1}{2}k\theta^2 \quad (7)$$

where v is the speed when the vehicle starts braking, k is the spring constant, and θ is the twisting angle of the torsion spring. From Equation (7), greater vehicle speed (v) and mass (M) result in a larger twisting angle of the torsion spring. This conclusion is further supported by an analysis of the change of momentum (ΔP) and impulse (ΔJ) during the braking period. Since the final speed (v_f) of the vehicle equals zero, the following equations may be derived as:

$$\Delta P = M\Delta v = Mv_f - Mv_i = -Mv \quad (8)$$

$$\Delta J = F\Delta t = -Mv \quad (9)$$

where F is the average deformation force with which the wingnut twists the spring during the braking period and Δt is the duration for which the spring is twisted. Equation (9) shows that to reduce the deformation force while maintaining high speed, the vehicle mass must be reduced since the braking period (Δt) keeps constant when the same spring is used.

The CG distance from the front axle can be calculated by center of mass equation:

$$X_{CM} = \frac{\sum m_i x_i}{M} = \frac{507(14) + m_{load}(D)}{507 + m_{load}} \quad (10)$$

Where, m_{load} is 120, 240, 360, 480, and 600 grams and D is the distance (cm) from the front axle, 3.1 (front), 14.8 (middle) and 33 (rear) (Table 1).

This study shows that a vehicle with a rearward center of gravity and a medium mass result in greatest speed and braking accuracy. The results of this study can be applied to the future design of gravity vehicles with consideration of their centers of gravity and mass. Further investigation will be needed in order to translate the results of this study to large scale automobiles.



Figure 6: Braking System Composed of Wingnut Geared with Torsion Spring at a Specific Point. (A) The vehicle decelerates when the wingnut starts to gear with the torsion spring. (B) The vehicle stops moving when a static equilibrium between the rotational torque of the wingnut and the twisting torque of the torsion spring is established.

MATERIALS & METHODS

Materials and Construction of Gravity Vehicle

Figures 5A and 5B are sketches of the ramp and vehicle drawn with SOLIDWORKS 3D CAD Software (10), in which a trigger was installed at the top of the ramp. A Gravity Vehicle device was built to meet the requirements, in which a ramp has a 49.5 cm x 49.5 cm base and a height of 99.8 cm, and a vehicle has a length of 36 cm and a width of 24 cm (Figure 5C). The ramp was built with fiberboard, pine and poplar wood boards bound by wood glue and nails. All ramp materials were purchased from Home Depot. The vehicle was built with 4 Banebots wheels, a basswood chassis, a braking system, a dowel, wood mounts, and other parts. A wingnut, Teflon and rubber washers, a U-bolt plate, threaded axles, and compression springs were purchased from Ace Hardware. Wheels and shafts were purchased from BaneBots LLC. Miniature ball bearings were purchased from NationSkander California Corporation. Torsion springs were purchased from Grainger Industry Supply. A digital balance and stopwatch timer were purchased from Walmart. A push button spring latch used as the trigger mechanism was bought on Amazon and installed at the top of the ramp. The braking system was built with a wingnut and torsion spring. The wingnut moved along the threaded axle from left to right for a predetermined length based on the target distance. The torsion spring was installed with its coils concentric to a metal pin situated adjacent to the front axle so that a leg of the spring could gear with the wingnut at a specific point. The vehicle decelerated when the wingnut started to press the torsion spring (Figure 6A) and came to a full stop when a static equilibrium between the translational force of the wingnut and the deflection force of the spring was established (Figure 6B). If the elastic limit of the spring was exceeded, the spring was replaced with a stronger one.

Experimental Procedure

The target was set at 10.50 meters, halfway between 9.00

and 12.00 meters, in all experiments. To reduce systematic errors, each run was performed on the same wood floor. The vehicle rolls down from the top of the ramp and then across on the wood floor until the vehicle brakes at the target. The running time was measured by stopwatch from the launch to the vehicle stop. The average running time and braking distance were calculated by running three trials under the same conditions. The mass load was located on the center line and secured with duct tape to prevent movement during the run. In front loading, the distance between the center of the mass load and front axle was measured as 3.1 cm, 14.8 cm in the middle loading, and 33.0 cm in the rear loading.

Center of Gravity Modelling

Recent research by Patel *et al.* proposed a fast and practical method to determine the three-dimensional CG of any symmetric or asymmetric vehicle. By using force restoration technology and flexure pivots, all three axes of CG could be measured in a single setup with the accuracy up to 10 millimeters (11). Their method helped us develop the CG measuring practices in this study.

For the gravity vehicle, a simplified model for determining the CG location was constructed (Figure 7). Due to its symmetric and low-height design, only CG locations along the longitudinal direction were considered for calculation. As the load was moved rearwards, the CG also shifted rearwards. If the two front wheels were placed on a balance while the two rear wheels were supported in the same horizontal plane, the normal force F_A exerted by the balance could be measured (Figure 7A). Switching the balance to the two rear wheels could yield the normal force F_B (Figure 7B). After measuring the two parameters F_A and F_B , the CG location could be calculated based on static equilibrium and Newton's second law. Once the CG position was determined, the height with which the vehicle was launched could also be obtained. Using this value, the approximate speed was calculated by the Law of Energy Conservation. Insight was thus gained on the effect

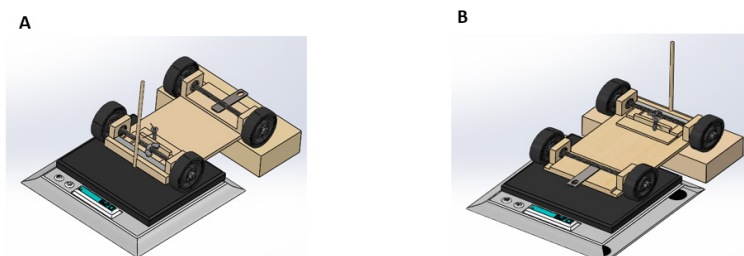


Figure 7: Simplified Vehicle Model for Determining the CG location. (A) The balance measures the normal force F_A on the front wheels. (B) The balance measures the normal force F_B on the rear wheels.



Figure 8: Diagram of Force Analysis. (A) The mass load (F_C) is located between the two fulcrums. F_A is the normal force from the front wheels, F_B the normal force from the rear wheels, and F_{CG} is the gravitational force at the CG. a is the distance of F_{CG} from the fulcrum A, b is the distance of F_{CG} from the fulcrum B, and c is the distance of F_C from the fulcrum B. (B) The mass load (F_C) is located behind the fulcrum B. All symbols are same as those of (A).

of the optimal CG position on speed and accuracy.

When the load is placed onto the vehicle, there are two scenarios: the load is located between two fulcrums A and B corresponding to front and middle loadings or the mass load is outside fulcrum B (**Figure 8**). In either case, the force equilibrium leads to the following equations based on Newton's second law:

$$F_{CG} + F_C = F_A + F_B \quad (11)$$

$$F_{CG} = F_A + F_B - F_C \quad (12)$$

Here, F_C is the gravity force from the mass load and F_A and F_B are measured by the balance. F_{CG} can be calculated from Equation (12). When the mass is located between the two fulcrums A and B, in terms of the torque equilibrium, two equations can be deduced as:

$$\text{For fulcrum B: } (a + b)F_A = bF_{CG} + cF_C \quad (13)$$

$$\text{For fulcrum A: } aF_{CG} + F_C(a + b - c) = F_B(a + b) \quad (14)$$

When the mass load is located outside fulcrum B, the two equations can be expressed as:

$$\text{For fulcrum B: } F_A(a + b) + cF_C = bF_{CG} \quad (15)$$

$$\text{For fulcrum A: } F_C(a + b + c) + aF_{CG} = F_B(a + b) \quad (16)$$

In either case, the distance a of the CG position from the dowel can be calculated from the combination of Equations (13) and (14) or Equations (15) and (16), since there are only two unknowns, a and b . The symbol c is the measured distance between the center of the mass load and fulcrum B.

Numerical Analysis

The optimal mass (867 grams) of the vehicle with a load outside of fulcrum B was taken as an example. From the measurements of F_A (1.92 N), F_B (10.18 N), and F_C (3.53 N), F_{CG} was calculated as:

$$F_{CG} = F_A + F_B - F_C = 8.57 \quad (17)$$

Introducing F_A (1.92 N), F_B (10.18 N), F_C (3.53 N), F_{CG} (8.57 N), and c (2.4 cm) into Equations (14) and (15), they were simplified as:

$$a + b = 29.6 \quad (18)$$

$$a - 3.46b = -4.41 \quad (19)$$

Solving the two-variable equations yielded a as 22.3 cm. The standard deviation was 22 ± 1 cm from the front axle.

The unloaded vehicle (507 grams) was taken as an example. From the measurements of F_A (2.65 N) and F_B (2.32 N), F_{CG} was calculated as 4.97 N from equation (12) since F_C was zero. Introducing F_A (2.65 N), F_B (2.32 N) and F_{CG} (4.97 N), as well as $F_C = 0$ and $c = 0$ into Equations (13) and (14), the distance a was calculated as 14.0 cm. After rear loading, the CG position was shifted rearward to 11 cm, which led to a greater than 20% speed increase (**Table 1**).

The height of the unloaded vehicle was 73 cm, so the height of the rear-loaded vehicle was 81 cm. Since m is approximately equal to M in Equation (5), the speed was approximated as 3.12 m/s for the unloaded vehicle by introducing the height of 73 cm. Similarly, the approximate speed of rear-loaded vehicle was found to be 3.25 m/s by introducing the height of 81 cm. Compared to the theoretical calculations, the experimental data, 2.39 m/s (unloaded) and 3.00 m/s (867 grams, rear loading) are smaller due to energy loss (**Table 1**). The larger speed difference between 2.39 m/s and 3.00 m/s and accuracy difference between 20.4 m⁻¹ and 38.5 m⁻¹ exemplified that the rearward shift of the CG position greatly improved the vehicle's performance.

ACKNOWLEDGEMENTS

We would like to express our heartfelt gratitude to Mr. Donald Terek, a retired engineer, for his help during the construction of the gravity vehicle device. We would also like to thank Mr. Mike Farrell, who allowed us to use the gym facilities at California State University, Fullerton for experimental studies.

Received: October 5, 2020

Accepted: December 11, 2020

Published: March 16, 2021

REFERENCES

1. Mazumder, H., *et al.* "Performance Analysis of EV for Different Mass Distributions to Ensure Safe Handling." *Energy Procedia*, vol. 14, Dec. 2012, pp. 949-954., doi:10.1016/j.egypro.2011.12.1038.
2. Rievaj, V., *et al.* "The Effects of Vehicle Load on Driving Characteristics." *Advances in Science and Technology Research Journal*, vol. 12, no. 1, Mar. 2018, pp. 142-149. doi: 10.12913/22998624/80896.
3. Skrucany, T., *et al.* "Impact of Cargo Distribution on the Vehicle Flatback on Braking Distance in Road Freight Transport." *MATEC Web of Conferences*, 18th International Scientific Conference-LOGI, vol. 134, 2017, pp. 54. doi: 10.1051/mateconf/201713400054.

4. Skrucany, T., *et al.* "The Influence of the Cargo weight and its Position on the Braking Characteristics of Light Commercial Vehicles." *Open Engineering*. vol. 10, no. 1, Feb. 2020, pp. 154-165., doi: 10.515/eng-2020-0024.
5. Mehmet, A., *et al.* "Method for Determining the Centre of Gravity for an Automotive Vehicle." WO 2007/098891A1. <https://patents.google.com/patent/WO2007098891A1/en>.
6. Lee, J. H., *et al.* "Real-time Longitudinal Location Estimation of Vehicle Center of Gravity." *International Journal of Automotive Technology*, vol. 19, no. 4, Jun. 2018, pp. 651-658.
7. Science Olympiad Division C Rules Manual. Gravity Vehicle, 2020, pp. 30-32. http://api-static.ctlglobalsolutions.com/science/Science_Olympiad_Div_C_2020_Rules_Manual_Web.pdf.
8. Yutaka Nishiyama "The Brachistochrone Curve: The Problem of Quickest Descent." *International Journal of Pure and Applied Mathematics*, vol. 82, no. 3, Sep. 2013, pp. 409-419. <https://ijpam.eu/contents/2013-82-3/8/8.pdf>
9. Krishna, K. R., *et al.* "Kinetic Energy Storage and Recovery System using Torsion Spring." *International Journal of Engineering Research & Technology*, vol 3, no. 22, 2015, pp. 1-4, Special Issue. www.ijert.org/research/kinetic-energy-storage-and-recovery-system-using-torsion-spring-IJERTCONV3IS22029.pdf.
10. 3D CAD Design Software, Dassault Systems Solidworks Student Edition, 2019.
11. Patel, S. G., *et al.* "Measuring a Centre of Gravity of an Object using 4 Load Transducer Method." *International Journal for Innovative Research in Science & Technology*, vol. 6, no. 1, Jan. 2017, pp. 210-214., doi:10.17577/IJERTV6IS010100.

Copyright: © 2021 Tian and Whitfield. All JEI articles are distributed under the attribution non-commercial, no derivative license (<http://creativecommons.org/licenses/by-nc-nd/3.0/>). This means that anyone is free to share, copy and distribute an unaltered article for non-commercial purposes provided the original author and source is credited.